J Sol-Gel Sci Technol (2013) 68:278–283
DOI 10.1007/s10971-013-3164-9

ORIGINAL PAPER

Long-lived emission from Eu^{3+}:PbF_2 nanocrystals distributed into sol–gel silica glass

Barbara Szpikowska-Sroka · Lidia Żur · Rozalia Czoik · Tomasz Goryczka · Andrzej S. Swinarew · Maria Żądło · Wojciech A. Pisarski

Received: 18 April 2013 / Accepted: 23 September 2013 / Published online: 28 September 2013

Abstract This paper reports an optical investigation of Eu^{3+}:PbF_2 nanocrystals distributed into silica glasses fabricated by sol–gel methods. The sample microstructure was investigated using scanning transmission electron microscopy. The β-cubic PbF_2 crystalline phase was identified using X-ray diffraction analysis. The observed emission bands correspond to $^5D_0 \rightarrow {}^7F_J$ (J = 0–4) transitions of Eu^{3+}. The spectroscopic parameters for Eu^{3+} ions were determined based on excitation and emission measurements as well as luminescence decay analysis. Emission originating from $^5D_0$ state of Eu^{3+} ions in sample containing PbF_2 nanocrystals is long-lived in comparison to precursor sol–gel silica glasses.

Keywords Nanocrystals · Europium ions · Sol–gel method · Glass ceramics · Luminescence properties

1 Introduction

In recent years rare earth doped glass materials have been extensively investigated due to their interesting optical properties and applications in optoelectronics. The trivalent europium ions due to orange/red emission are one of the most important of the rare earth ions and can be applied in solid-state laser, plasma display panel or spectroscopic probe [1–5]. Oxyfluoride glass–ceramics based on the silicate glassy matrix are unique class of materials that combine the advantages of physical and chemical properties of an oxide glass with the high solubility of the rare earth ions. Moreover, the low phonon energy of fluoride crystalline phase is very importance because the higher phonon energy of the host is related to the higher non-radiative transition probability, which will result in decrease of luminescence efficiency [6–9]. Furthermore, the glass–ceramics stay at intermediate state between crystalline materials and glasses, so that they combine the best properties of crystals (high emission, quantum yield of luminescence, mechanical and thermal strength, etc.) and glasses (possibilities of pressing and molding, pulling optical fibers, etc.).

Melt quenching method is well known as conventional method used to obtain glass–ceramic systems. However, the composition of glasses is uncertain due to partial evaporation of some components during high temperature melting. Sol–gel method provides a new approach to prepare glass–ceramics [10]. Compared to the conventional melt quenching method several advantages have been observed, such as: lower processing temperature, easier composition control, better homogeneity of the product, and wide range of compositions. The heat treatment process is a significant step in this method which allows to the removal of the remaining hydroxyl groups which can suppress the luminescence. During heat treatment process close to the crystallization temperature the oxyfluoride glass–ceramics can be obtained, in which fluoride crystallites are dispersed in the amorphous matrix and rare earth ions are usually incorporated into crystalline phase. If europium ions are incorporated into crystal phase, longer fluorescence lifetime of excited state is exhibited as well as relative emission band intensities of Eu^{3+} are completely

B. Szpikowska-Sroka (✉) · L. Żur · R. Czoik · M. Żądło · W. A. Pisarski
Institute of Chemistry, University of Silesia, 9 Szkolna Street, 40-007 Katowice, Poland
e-mail: barbara.szpikowska-sroka@us.edu.pl

T. Goryczka · A. S. Swinarew
Institute of Materials Science, University of Silesia, Bankowa 12, 40-007 Katowice, Poland

different. In the literature there are many published works on the emission properties of Eu^{3+}, some of them are concentrated on the sol–gel synthesis and preparation of europium doped fluoride nanocrystals (e.g. $NaYF_4$, CaF_2, BaF_2, LaF_3, YF_3, $LiGdF_4$) using heat treatment process [11–16]. To the best of our knowledge, only a few works are available on the Ln^{3+}:PbF_2 particles, for example PbF_2 nanocrystals containing ytterbium, erbium, holmium and thulium [17, 18]. There are no reports on the preparation of Eu^{3+}-doped PbF_2–SiO_2 glass system by sol–gel method and fabrication of Eu^{3+}:PbF_2 nanocrystals. Their optical properties are not documented. These facts were sufficient to carry out research on the Eu^{3+}:PbF_2 fluoride nanocrystals distributed into sol–gel silica glass.

In this Letter, we present new optical results for sol–gel silica glasses doped with Eu^{3+} ions before and after heat treatment. Structural and optical changes around Eu^{3+} were examined using scanning transmission electron microscopy (STEM), X-ray diffraction (XRD) and emission measurements.

2 Experimental

The reagents used in the synthesis of the sol–gel silica glasses were of analytical grade and supplied by Aldrich Chemical Co. Deionized water obtained from Elix 3 system (Millipore, Molsheim, France) was used during the experiments.

Glasses with the following composition $9.9TEOS - 19.8C_2H_5OH - 39.6H_2O - 19.8DMF–3.9HNO_3 - 1.1(Pb(CH_3COO)_2 + Eu(CH_3COO)_3) - 5.9CF_3COOH$, in molar % were prepared by sol–gel methods based on procedure [19]. The solution of tetraethoxysilane (TEOS) and *N*,*N*-dimethylformamide (DMF) in ethanol and water with nitric acid as a catalyst was hydrolyzed for 30 min at room temperature to make sure that all components were totally mixed. Subsequently, $Pb(CH_3COO)_2$ and $Eu(CH_3COO)_3$ were dissolved in water with trifluoroacetic acid and added dropwise into the first solution. Obtained transparent solution was stirred during 5 h at room temperature. A wet-gel was obtained by leaving the solution in a sealed container at 35 °C for 5–6 weeks. This step was required in order to obtain dried samples, known as xerogels (denoted as SG-Eu). Finally, these xerogels were inserted into cold furnace (FCF 5 5SHP produced by Czylok Poland) and heat treated, at 350 °C for 10 h, according to data reported in the literature about PbF_2 nanocrystals [4, 6, 17–19], in order to precipitate nanocrystallites in controlled size, giving rise to a transparent glass–ceramic (denoted as SG-Eu-HT). The temperature of furnace was raised with heating rate of 10 °C min^{-1}, the annealing process was carried out in air. After annealing the samples were cooled to room temperature in a closed furnace. The resulting system is composed of an amorphous oxide sol–gel matrix with Eu^{3+}:β-PbF_2 crystallites embedded into it.

The microstructures of the samples containing PbF_2 crystallites were studied using a scanning transmission electron microscopy (STEM, Hitachi HD-2300A) equipped with an energy dispersive X-ray spectroscope (EDS). The sol–gel glass samples before and after heat treatment were examined using X-ray diffraction (X'Pert X-ray diffractometer). Luminescence spectra were performed using Horiba Jobin–Yvon spectrofluorimeter FLUOROMAX-4 with 150 W xenon lamp as light source. The measurements were carried out with a spectral resolution of 0.1 nm without smoothing and correction. The emission spectra were registered in range 550–750 nm upon excitation at 393 nm, whereas the excitation spectra were recorded in the 350–500 nm spectral ranges ($\lambda_{em} = 611$ nm). Luminescence decay curves were detected at the same conditions with accuracy of ±2 μs. All experiment and spectral measurements were carried out at room temperature ($T = 20 \pm 2$ °C).

3 Results and discussion

3.1 Structural properties

Qualitative chemical analysis and structural properties of the sol–gel samples were studied using microscopic methods and X-ray diffraction measurements. The microstructure was characterized qualitatively by scanning transmission electron microscopy (STEM). The micrograph of sol–gel sample after annealing process is presented in Fig. 1. The STEM image shows 4–6 nm sized nanoparticles (a), which are distributed into sol–gel silica glass matrix (b). The energy dispersive X-ray spectroscopic measurements (EDS) were also used for the analysis of chemical composition. The EDS spectra with nanosized probe taken from (a) an individual nanoparticle and (b) from the sol–gel glass matrix were registered, respectively. They are presented in Fig. 2. Detailed qualitative analysis using EDS technique reveals that several peaks related to Si, Pb, O and F were detected. Moreover, the additional Cu, Al and C signals also appeared. The peaks of Cu and Al are coming from the STEM holder construction. The holder consists of copper mesh on which the samples were located. The copper mesh was held by the aluminum bracket. The presence of peak related to carbon is a result of contamination process. However, the most important information is that the spectrum from the nanoparticle (a) exhibits quite strong F and Pb signals denoted as (*) in contrast to the spectrum for the sol–gel silica glass (b), where some peaks due to Si, Pb and O are mainly observed.

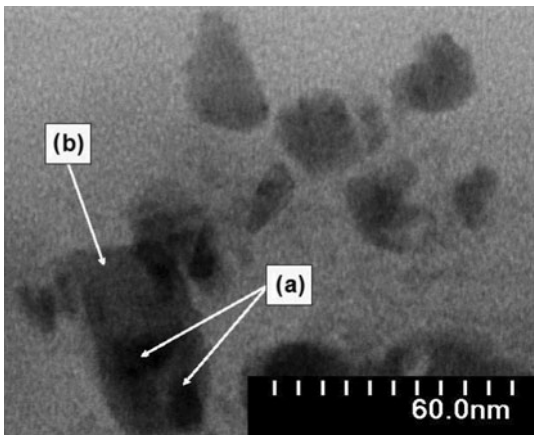

Fig. 1 STEM image of PbF_2 nanoparticles distributed into sol–gel silica glass matrix

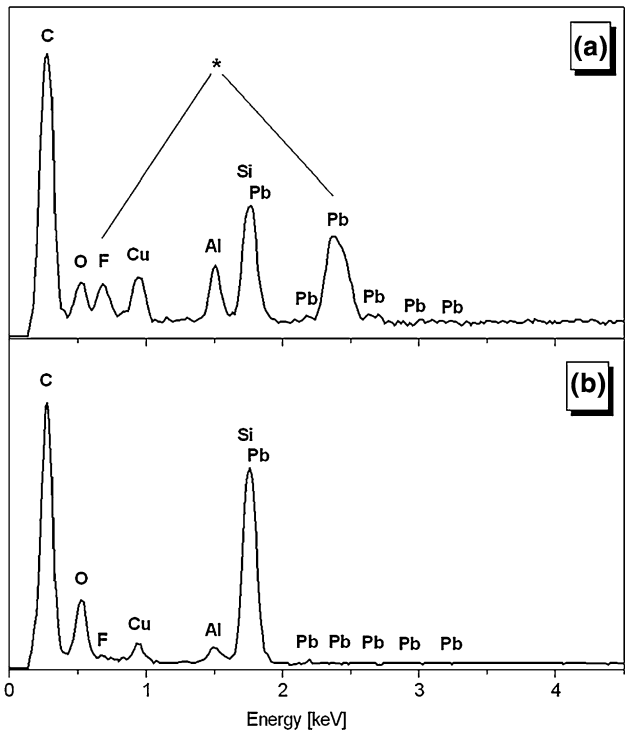

Fig. 2 EDS spectra with nanosized probe taken from **a** individual nanoparticle and **b** from the sol–gel silica glass matrix

These peaks are attributed to the glass matrix surrounding the nanoparticles. All these confirmed further that PbF_2 nanoparticles were formed in the annealing process.

X-ray diffraction was used to confirm the nature of the studied samples. Figure 3 shows XRD patterns for sol–gel silica glass samples before and after heat treatment. It was found that the studied systems before heat treatment were fully amorphous, without any crystallization peaks. Interesting results have been obtained when the samples were annealed at controlled temperature and time. After heat

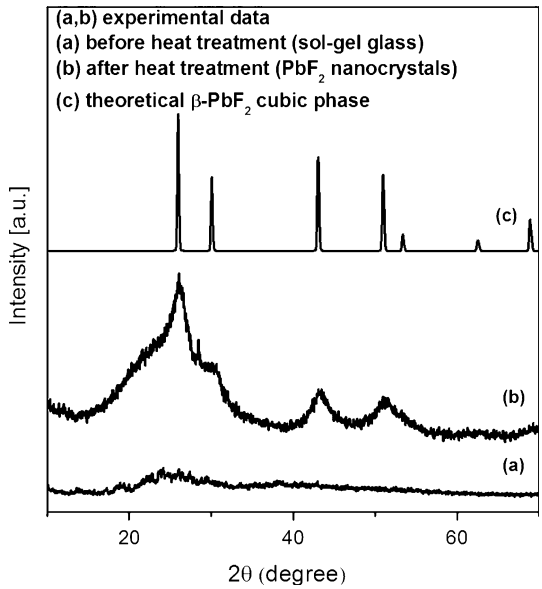

Fig. 3 X-ray diffraction patterns for sol–gel silica glasses before and after heat treatment and theoretical XRD pattern of cubic PbF_2

treatment in the spectra were observed several broad peaks. Based on theoretical XRD pattern they are assigned to cubic β-PbF_2 crystalline phase. Crystal sizes have been estimated from XRD by using Scherrer's equation ($D = K\lambda/\beta\cos\theta$, where D is the crystal size, λ is the wavelength of X-ray, θ is the diffraction angle, β is the half width of the diffraction peak and K is a constant which value is 1). The particle size of PbF_2 crystallites was calculated from FWHM as an average from all diffraction lines. The mean value was 5 nm. Moreover, the crystallite size was re-examined with the Williamson-Hall formula, which includes internal stress influence on the line broadening. Also these calculations were done over all diffraction patterns. The lattice deformation was lower than 0.00007 % and the estimated particle size was 5.1 nm and is in very good agreement with the results obtained by Scherrer's methods.

3.2 Excitation and luminescence properties

The emission and excitation spectra for Eu^{3+} in sol–gel glasses before and after heat treatment are presented in Fig. 4. The excitation spectra was monitored at $\lambda_{em} = 611$ nm ($^5D_0 \rightarrow {}^7F_2$ red transition of Eu^{3+}) in the range from 350 to 500 nm. The main observed peaks correspond to Eu^{3+} transitions coming from the ground level $^7F_0$ to the $^5L_6$ and $^5D_2$ excited states of Eu^{3+}. The most intense excitation peak observed at 393 nm is due to $^7F_0 \rightarrow {}^5L_6$ transition. Emission spectrum of Eu^{3+} ions in sol–gel glasses has been recorded upon excitation of $^5L_6$ state at 393 nm pumped by the Xe lamp. For pumping in the $^5L_6$ state of Eu^{3+} the $^5D_3$, $^5D_2$, $^5D_1$, and $^5D_0$ levels are

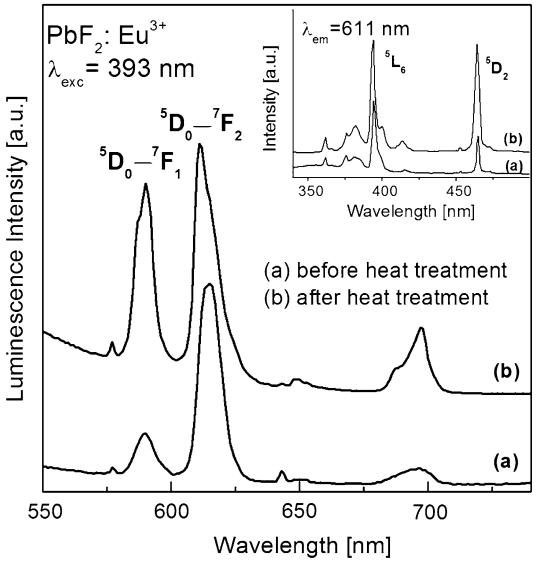

Fig. 4 Emission spectra of Eu^{3+} ions in sol–gel glasses before and after heat treatment. *Inset* shows excitation spectra monitored at 611 nm

populated, but owing to the small energy gaps between these levels the excitation energy is fast transferred in non-radiative way and we can observed the emission from the $^5D_0$ state of Eu^{3+} ions.

The emission spectra were registered in range 550–750 nm. Five-group emission lines located at 577, 590, 611, 643 and 697 nm, due to $^5D_0 \rightarrow {}^7F_J$ (J = 0, 1, 2, 3, 4) transition were observed, respectively.

It is well known that the luminescence intensity ratio R of $I(^5D_0 \rightarrow {}^7F_2)/I(^5D_0 \rightarrow {}^7F_1)$ (emission intensity of red line to the orange line) is a sensitive function of the local asymmetry around the optically active dopant (Eu^{3+} ions). This ratio can be modulated by varying the glass host composition, activator concentration and heat treatment. R value strongly depends on the surrounding rare-earth ions, which is drastically changed after heat treatment process. Small R value is usually attributed to higher local symmetry for Eu^{3+} ions. The increase in R value is due to increasing asymmetry and degree of covalency bonds. The $^5D_0 \rightarrow {}^7F_1$ line is magnetic dipole transition located at 590 nm, the intensity of this line is considered to be almost independent of the local symmetry. The $^5D_0 \rightarrow {}^7F_2$ line is an electric dipole transition located at 611 nm, the intensity of this line is dependent of the local field strength or hosts. As it is known, the probability of this electric dipole transition is higher for ions residing in asymmetric environment, while it is inhibited for ions close in symmetric surrounding. In studied samples before heat treatment the strongest emission was observed at 611 nm. Quite different situation was observed after annealing, the intensity of $^5D_0 \rightarrow {}^7F_2$ is comparable to the $^5D_0 \rightarrow {}^7F_1$ transitions. The luminescence intensity ratios R for glass samples before and after heat treatment have been decreased more than three times and are equal to 4.92 and 1.58, respectively (Table 1).

Table 1 Spectroscopic Parameters for Eu^{3+} Ions

Sample	Transition	λ_{em} (nm)	R	τ_m (ms)
SG-Eu	$^5D_o \rightarrow {}^7F_2$	611	4.92	0.49
	$^5D_o \rightarrow {}^7F_1$	590		
SG-Eu-HT	$^5D_o \rightarrow {}^7F_2$	611	1.58	2.71
	$^5D_o \rightarrow {}^7F_1$	590		

R Luminescence intensity ratio of $I(^5D_0 \rightarrow {}^7F_2)/I(^5D_0 \rightarrow {}^7F_1)$

τ_m Luminescence lifetime for the $^5D_0$ level of Eu^{3+} ions

The high value of the luminescence intensity ratio before annealing suggests that Eu^{3+} ions are located in a low symmetry site in amorphous silica matrix. After heat treatment, local symmetry around the optically active dopant (Eu^{3+} ions) and participation of ionic bonds increased [20]. The value of R is decreased due to incorporation of RE^{3+} ions into cubic β-PbF_2 crystalline phase. During heat treatment occur two simultaneously processes: reduction of OH groups and formation of fluoride nanocrystals. Reduction of OH groups results in increasing of luminescence intensity and lifetime. However, decreased of R value is due to change the environment of optically active dopant. The covalence oxide surroundings of europium ions changed to more ionic, due to presence of fluoride ions around active dopant. Changes in the environment around the europium ions and character of bonding between europium ions and surrounding ligands after annealing process may also indicate differences in the shape (narrowing and sharpening) of the emission bands, Fig. 4. Moreover, the RE^{3+} contribution in nanocrystals or in matrix was examined by other research groups, such as de Pablos-Martin et al. [7, 9], Bensalem et al. [21] and Armellini et al. [22]. Our results from luminescence spectra are in good agreement with data obtained by referred authors.

The relationship between the intensity ratio R and the covalent/ionic character of bonding between Eu^{3+} and surrounding ligands has been analyzed in detail by Khan et al. [2], Santana-Alonso et al. [11] and Bensalem et al. [21]. The values of R parameters obtained for glass sample containing PbF_2 nanocrystals presented in our work are in a good agreement with those estimated for other nanocrystalline fluoride-based systems, such as $NaYF_4$ [11] and PbF_2 obtained by traditional high-temperature melt-quenching technique [21].

The luminescence lifetime for the $^5D_0$ level of Eu^{3+} ions (Fig. 5) depends mainly on radiative probabilities of the $^5D_0 \rightarrow {}^7F_J$ transitions. The luminescence decay curves measured for samples before and after heat treatment were

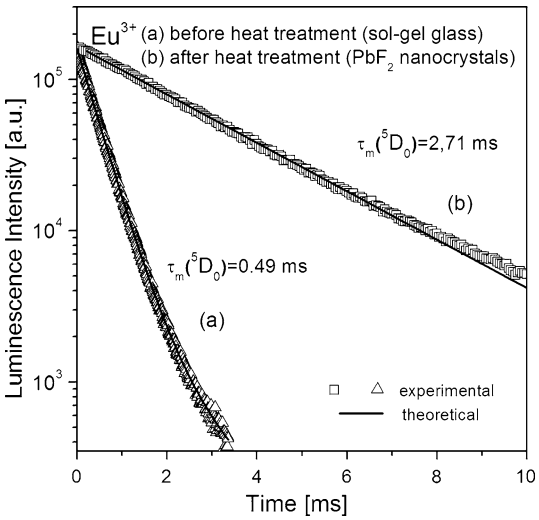

Fig. 5 The luminescence decay curves for $^5D_0$ state of Eu^{3+} ions in sol–gel glasses before and after heat treatment

very well fitted to single exponential function. The value of emission lifetime for Eu^{3+} increased five and half times, that is: 0.49 ms before heat treatment and 2.71 ms after heat treatment. Based on such large increase of lifetimes, we suppose that after heat treatment process part of europium ions were incorporated into crystalline phase. The relatively short emission lifetime in the sol–gel glass sample before heat treatment is due to the presence of high energy stretching vibrations of the residual hydroxyl groups, causing non-radiative decay mechanism, results in luminescence quenching. The concentration of the OH^- groups is significantly reduced during the heat treatment process resulting in a longer $^5D_0$ emission lifetime of Eu^{3+} ions incorporated into PbF_2 nanocrystals. The $^5D_0$ measured lifetime is similar to the value given by Secu et al. [12, 13] and by Bensalem et al. [21], but is much higher than value obtained by Khan et al. [2].

As pointed out above, the photoluminescence spectra and R ratio as well as their $^5D_0$ fluorescence lifetimes of europium ions doped to glass before and after heat treatment in examined systems are markedly different. It means that Eu^{3+} migrates from the glass to another phase upon ceramisation. Bensalem et al. [21] has identified this phase to be Eu^{3+}:β-PbF_2.

4 Conclusions

Optical properties of the Eu^{3+}-doped PbF_2–SiO_2 glasses obtained by sol–gel method have been investigated. Based on excitation and emission measurements as well as luminescence decay analysis the spectroscopic parameters for europium ions were determined. It was found that the control heat treatment process caused greatly increase of the luminescence lifetimes (from 0.49 to 2.71 ms) and significant decrease of luminescence intensity ratios R (from 4.92 to 1.58). Longer luminescence lifetimes is resultant of OH group reduction and PbF_2 nanocrystals formation. Such large differences at spectroscopic parameters may be caused mainly by changes in the environment around the optically active dopant and character of bonding between Eu^{3+} and surrounding ligands. It was found that the control annealing process allows obtained Eu^{3+}:PbF_2 nanocrystals distributed into sol–gel silica glasses, which results in changing of optical properties mentioned above. The sample microstructure was studied using scanning transmission electron microscopy. The β-cubic PbF_2 crystal phase was identified using X-ray diffraction.

References

1. Jacobsohn LG, Kucera CJ, James TL, Sprinkle KB, DiMaio JR, Kokuoz B, Yazgan-Kukouz B, DeVol TA, Ballato J (2010) Materials 3:2053–2068
2. Khan AF, Yadav R, Singh S, Dutta V, Chawla S (2010) Mater Res Bull 45:1562–1566
3. Dejneka MJ (1998) J Non-Cryst Solids 239:149–155
4. Bueno LA, Gouveia-Neto AS, da Costa EB, Messaddeq Y, Ribeiro SJL (2008) J Phys Condens Matter 20:145201
5. Fujihara S (2010) Sol-gel route to inorganic fluoride nanomaterials with optical properties. In: Tressaud A (ed) Functionalized inorganic fluorides: synthesis, characterization & properties of nanostructured solids. Wiley, New York
6. Sarkar S, Hazra C, Chatti M, Sudarsan V, Mahalingam V (2012) RSC Adv 2:8269–8272
7. de Pablos-Martín A, Duran A, Pascual MJ (2011) International materials reviews imr 175.3d
8. Bensalem C, Mortier M, Vivien D, Gredin P, Patriarche G, Diaf M (2012) N J Glass Ceram 2:65–74
9. de Pablos-Martin A, Durán A, Pascual MJ, Soria S, Righini GC, Ramírez MO, Bausá LE, Ristic D, Ferrari M, Höche T (2011) Proc SPIE. doi:10.1117/2.1201111.003940
10. Reisfeld R (1996) Struct Bond 85:99–147
11. Santana-Alonso A, Yanes AC, Méndez-Ramos J, del Castillo J, Rodríguez VD (2010) J Non-Cryst Solids 356:933–936
12. Secu M, Secu CE, Ghica C (2011) Opt Mater 33:613–617
13. Secu CE, Secu M, Ghica C, Mihut L (2011) Opt Mater 33:1770–1774
14. Yanes AC, Del-Castillo J, Méndez-Ramos J, Rodríguez VD, Torres ME, Arbiol J (2007) Opt Mater 29:999–1003
15. Yanes AC, Santana-Alonso A, Méndez-Ramos J, del Castillo J, Rodríguez VD (2011) Adv Funct Mater 21:3136–3142
16. Lepoutre S, Boyer D, Fujihara S, Mahiou R (2009) J Mater Chem 19:2784–2788
17. del Castillo J, Yanes AC, Méndez-Ramos J, Tikhomirov VK, Moshchalkov VV, Rodríguez VD (2010) J Sol-Gel Sci Technol 53:509–514

18. del Castillo AJ, Yanes AC, Méndez-Ramos J, Tikhomirov VK, Rodríguez VD (2009) Opt Mater 32:104–107
19. Luo W, Wang Y, Bao F, Zhou L, Wang X (2004) J Non-Cryst Solids 347:31–38
20. de Pablos-Martín A, Ristic D, Bhattacharyya S, Höche T, Mather GC, Ramírez MO, Soria S, Ferrari M, Righini GC, Bausá LE, Durán A, Pascual MJ (2013) J Am Ceram Soc 96:447–457
21. Bensalem C, Mortier M, Vivien D, Diaf M (2011) Opt Mater 33:791–798
22. Armellini C, Chiappini A, Chiasera A, Ferrari M, Jestin Y, Mortier M, Moser E, Retoux R, Righini GC (2007) J Nanomater 84745. doi: 10.1155/2007/84745